Journal of Alloys and Compounds 509 (2011) 769–774

Contents lists available at ScienceDirect

Journal of Alloys and Compounds

journal homepage: www.elsevier.com/locate/jallcom

The first-principles calculations for the elastic properties of Zr_2Al under compression

Xiao-Li Yuan[a,b], Dong-Qing Wei[b,d,*], Xiang-Rong Chen[a,c,**],
Qing-Ming Zhang[d], Zi-Zheng Gong[e]

[a] College of Physical Science and Technology, Sichuan University, Chengdu 610064, China
[b] College of Life Science and Biotechnology and Research Center Astronautics and Shanghai Jiaotong University, Shanghai 200240, China
[c] International Centre for Materials Physics, Chinese Academy of Sciences, Shenyang 110016, China
[d] State Key Laboratory of Explosion Science and Technology, Beijing Institute of Technology, Beijing 100081, China
[e] Chinese Academy of Space Sciences, Beijing 100094, China

ARTICLE INFO

Article history:
Received 10 May 2010
Received in revised form
14 September 2010
Accepted 18 September 2010
Available online 25 September 2010

Key words:
Elastic properties
Electronic band structure
Density functional theory
Zr_2Al

ABSTRACT

The first-principles calculations were applied to investigate the structural, elastic constants of Zr_2Al alloy with increasing pressure. These properties are based on the plane wave pseudopotential density functional theory (DFT) method within the generalized gradient approximation (GGA) for exchange and correlation. The result of the heat of formation of Zr_2Al crystal investigated is in excellent consistent with results from other study. The anisotropy, the shear modulus, and Young's modulus for the ideal polycrystalline Zr_2Al are also studied. It is found that (higher) pressure can significantly improve the ductility of Zr_2Al. Moreover, the elastic constants of Zr_2Al increase monotonically and the anisotropies decrease with the increasing pressure. Finally, it is observed that Zr *d* electrons are mainly contributed to the density of states at the Fermi level.

1. Introduction

Group IV transition metal zirconium and its alloys are crucial materials for applications in the fields of aerospace, medical, and nuclear, where their high strength, light weight, corrosion resistance, and the nuclear absorption cross sections are of prime interest. Consequently, these materials are of scientific and technological interest in recent years [1]. A large number of theories and experiments on the glass-forming ability of binary or trinary zirconium-based alloys such as Zr–Cu–Ti (Ni, Al, Be, Nb, Fe) [2–10] have been reported. These zirconium-based alloys have been demonstrated to exhibit intriguing glass-forming ability and are currently the major species of bulk metallic glasses with extraordinary thermomechanical and electronomagnetic properties.

Particularly, Zr–Al based amorphous and nanocrystalline alloys have been paid much attention due to their high strength, high ductility, and high glass-forming ability [11,12]. Several investigations [13–16] on the solid solubility of Al in Zr were also reported. Wang et al. [17] analyzed the phase equilibrium and thermodynamic data of the Al–Zr using thermodynamic models. Alatalo et al. [18] calculated the heats of formation of a number of different Al–Zr possible structures using both all-electron and pseudopotential methods. Generally, the mechanical properties of the alloys can be greatly improved by controlling the crystallographic phases present, optimizing the microstructure of the material and external pressure. For example, the elastic constants play an important role in determining the strength of the alloy materials and the response of the crystal to external forces, which is characterized by bulk modulus, shear modulus, Young's modulus and Poisson's ratio, and elastic properties also related thermodynamically to the specific heat, thermal expansion, Debye temperature, and the Grüneisen parameter. Especially, bulk modulus, shear modulus and their derivatives as a function of pressure are also important parameters in understanding the structural behavior and physical properties of the alloy materials under compression. Although a large number of publications studied the metallic glasses based on alloy including Zr_2Al compound, the elastic properties and electronic band structure of Zr_2Al crystal under high pressure are rarely reported up to now.

---

* Corresponding author at: College of Life Science and Biotechnology and Research Center Astronautics and Shanghai Jiaotong University, Shanghai 200240, China.
** Corresponding author at: College of Physical Science and Technology, Sichuan University, Chengdu 610064, China.
E-mail addresses: dqwei@sjtu.edu.cn (D.-Q. Wei), x.r.chen@tom.com (X.-R. Chen).

0925-8388/$ – see front matter © 2010 Elsevier B.V. All rights reserved.
doi:10.1016/j.jallcom.2010.09.084

Therefore, investigating the Zr_2Al crystal.is essential for further understanding the metallic glasses.

In this study, we presented the first-principles calculations to investigate the properties of binary Zr_2Al crystal under high pressure. Lattice parameters, elastic properties and electronic band structure are investigated by applying the first-principles plane-wave method within the generalized gradient approximation correction (GGA) in the frame of density functional theory [19] based on the Cambridge Serial Total Energy Package (CASTEP) program [20,21]. In Section 2, the calculation method will be presented in detail. The theoretical result and some discussion are given in Section 3. Finally, conclusions are summarized.

2. Method of calculation

2.1. Total energy electronic structure calculations

The density functional theory (DFT) [22,23] has successfully been applied to the first-principles calculations of ground-state properties of various materials from the theoretical point of view [24,25]. In the DFT method, the GGA is widely used for the first-principles prediction of the ground-state properties of crystalline solids, and is known to give many of these properties to high accuracy. It can be successfully applied to estimate the accurate theoretical values of static structural properties, phonon spectra, crystal stability, and pressure-induced phase transformations in many solids. To investigate the elastic constants of a material theoretically from the first principles, the total energy of a crystal is calculated as a function of the unit cell deformations, which deals with the elastic constants under considerations [26].

In present calculation, we apply the GGA for the exchange-correlation functional in the scheme of Perdew–Burke–Ernzerhof (PBE) [19] to describe the exchange and correlation potential. Pseudo-atom calculations are performed for Zr ($4d^25s^2$) and Al ($3s^23p^1$). The electronic wave functions are expanded in a plane wave basis set with energy cut-off of 360 eV. The K-space integration has been performed using $9 \times 9 \times 8$ k-points in the irreducible Brillouin zone, where the self-consistent convergence of the total energy is 1.0×10^{-6} eV/Atom. This structure has been optimized by using the BFGS algorithm [27] for pressures ranging from −10 GPa to 100 GPa. We choose the same parameters in our electronic structure calculations and elastic properties calculations.

2.2. Elastic properties

The elastic constants are calculated as the second derivatives of the internal energy with respect to the strain tensor. They are defined by a Taylor expansion of the total energy $E(V, \delta)$ for the system with respect to a small strain δ of the lattice primitive cell volume V. The energy of a strained system is as follows [28,29]:

$$E(V,\delta) = E(V_0,0) + V_0\left(\sum_i \tau_i\xi_i\delta_i + \frac{1}{2}\sum_{ij} C_{ij}\delta_i\xi_j\delta_j\right) \tag{1}$$

where $E(V, 0)$ is the energy of the unstrained system with equilibrium volume V_0, τ_i is an element in the stress tensor and ξ_i is a factor to take care of Voigt index [29].

There are five independent components of the elastic tensor for Zr_2Al, i.e., C_{11}, C_{12}, C_{13}, C_{33} and C_{44}. For an hcp crystal under pressure, the generalized mechanical stability criteria [30] are as follows:

$$C_{12} > 0, \quad C_{33} > 0; \quad C_{66} = \frac{C_{11} - C_{12}}{2} > 0, \quad C_{44} > 0 \tag{2}$$

$$(C_{11} + C_{12})\ \ C_{33} - 2C_{13}^2 > 0 \tag{3}$$

The mechanical anisotropy of Zr_2Al can be calculated by using the bulk moduli B_a along the a-axis and B_c along the c-axis, which are defined as [31,32]:

$$B_a = a\frac{dP}{da} = \frac{\Lambda}{2+\alpha} \tag{4}$$

$$B_c = c\frac{dP}{dc} = \frac{B_a}{\alpha} \tag{5}$$

$$\Lambda = 2(C_{11} + C_{12}) + 4C_{13}\alpha + C_{33}\alpha^2 \tag{6}$$

$$\alpha = \frac{C_{11} + C_{12} - 2C_{13}}{C_{33} - C_{13}} \tag{7}$$

where α is defined as the relative change of the c-axis as a function of the deformation of the a-axis. By the above-mentioned equations, the linear bulk modulus can be obtained from our calculated single crystal elastic constants.

The Voigt and Reuss assumptions [33] result in the theoretical maximum and minimum values of the isotropic elastic modulus, respectively. The bulk modulus is an invariant by rotation and it does not depend on the crystal orientation. Therefore, the bulk modulus B for hexagonal Zr_2Al is presented by:

$$B = B_V = B_R = \frac{1}{9}\left[2(C_{11} + C_{12}) + C_{33} + 4C_{13}\right] \tag{8}$$

The upper and the lower bounds for the shear modulus of polycrystalline Zr_2Al aggregate according to Voigt and Reuss approximations are defined as follows:

$$G_V = \frac{1}{30}(C_{11} + C_{12} + 2C_{33} - 4C_{13} + 12C_{44} + 12C_{66}) \tag{9}$$

$$G_R = \frac{5}{2}\,\frac{[(C_{11} + C_{12})C_{33} - 2C_{13}{}^2]C_{66}C_{44}}{3B_V C_{66}C_{44} + [(C_{11} + C_{12})C_{33} - 2C_{13}{}^2](C_{66} + C_{44})} \tag{10}$$

where $C_{66} = 1/2(C_{11} - C_{12})$, and the Voigt–Reuss–Hill (VRH) averages for shear modulus (G) is defined as [34,35]:

$$G = \frac{G_V + G_R}{2} \tag{11}$$

The polycrystalline elastic modulus (E) and the Poisson ratio (σ) are then computed from these values using the following equations:

$$E = \frac{9BG}{3B + G}, \qquad \sigma = \frac{3B - 2G}{2(3B + G)} \tag{12}$$

3. Results and discussion

3.1. Structural properties and pressure effects

Zr_2Al is a hexagonal close-packed (hcp) structure with space group P63/mmc. Two Al atoms occupy the 2c Wyckoff site (1/3, 2/3, 1/4) and (2/3, 1/3, 3/4) and four Zr atoms occupy the 2a site (0, 0, 0), (0, 0, 1/2) and 2d site (1/3, 2/3, 3/4), (2/3, 1/3, 1/4) in a six atoms unit cell, respectively. Since the experimental lattice parameter ratio c/a is 1.211, we thus calculate a series of different c/a ratios from 1.196 to 1.228, with an interval of 0.004. For each c/a, a series of different values of lattice constant a are set to calculate the total energies E and the corresponding volumes V, and then an energy–volume (E–V) curve can be obtained by fitting the calculated E–V data to the Brich–Murnaghan of state (EOS) [36]:

$$\Delta E(V) = E - E_0 = B_0V_0\left[\frac{V_n}{B_0'} + \frac{1}{1 - B_0'} + \frac{V_n^{1-B_0'}}{B_0'(B_0' - 1)}\right] \tag{13}$$

where E_0 is the equilibrium energy at the zero pressure. The pressure P versus the normalized volume V_n is obtained through the

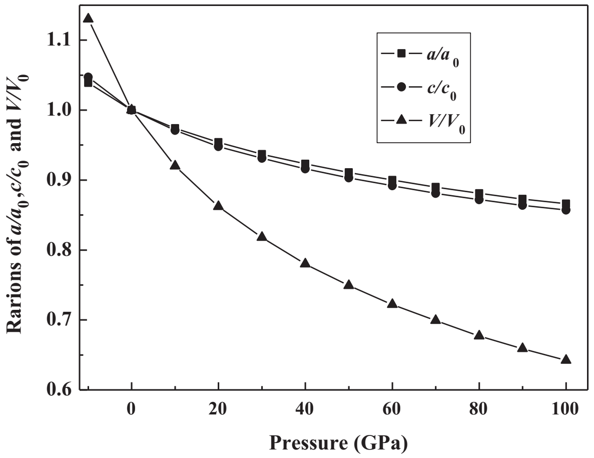

Fig. 1. The normalized lattice parameters a/a_0, c/c_0 and primitive cell volume V/V_0 as a function of pressure P for Zr_2Al at 0 K.

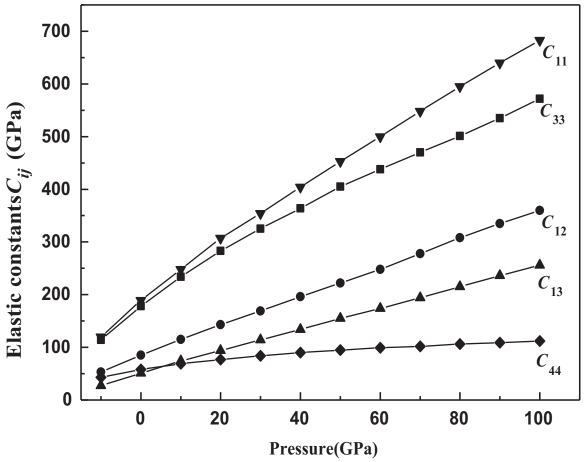

Fig. 3. The calculated elastic constants C_{ij} as a function of pressure P.

following thermodynamic equation:

$$P = -\frac{dE}{dV} = \frac{B_0}{B'_0}\left[V_n^{-B'_0} - 1\right] \tag{14}$$

It is found that the most stable structure of Zr_2Al at $P = 0$ and $T = 0$ corresponds to the ratio c/a of 1.208, and the calculated the zero pressure bulk modulus B_0 and its pressure derivative $B_0{}'$ are listed in Table 1, together with other experimental data [37], and we also list the bulk modulus B_0 and its pressure derivative $B_0{}'$ results of the Zr_2Al with CdI_2 structure [38] for comparison due to lacking of experimental or other theoretical results. These results are in excellent agreement with the experimental data [37] and other structure theoretical results [38].

We also investigate the heat of formation of Zr_2Al crystal. The heat of formation of Zr_2Al crystal calculated is −0.35 eV/atom (see Table 1). Unfortunately, there are no experimental values but it is in excellent consistent with results from other study [18] which obtains a value of −0.35 eV/atom by LASTO method and −0.37 eV/Aatom by PWPP method.

Fig. 1 shows the pressure dependence of the normalized lattice parameters a/a_0, c/c_0 and primitive cell volume V/V_0 in the range of from −10 to 100 GPa (where a_0, c_0 and V_0 are the zero pressure equilibrium structural parameters). As pressure increasing, the equilibrium ratio c/c_0 decreases more quickly than a/a_0, indicating that the compression along the c-axis is much larger than that along the a-axis. This result is in agreement with the comparatively weaker (Al–Zr) bonds which determine the c-axis length. Unfortunately, there are no experimental data compared with our data.

3.2. Elastic properties of the Zr_2Al

Elastic properties of the materials are very important because they related to various fundamental solid-state properties, such as equation of state (EOS), thermodynamically to the specific heat, thermal expansion, Debye temperature, melting point, Grüneisen parameter and so on. The elastic modulus determines the response of the crystal to external forces, as characterized by bulk modulus, shear modulus and Young's modulus, and plays a role in determining the strength of the materials. Table 2 presents the elastic constants of Zr_2Al at 0 K and 0 GPa. Since there is currently no experimental measurement of elastic constants, we show the experimental and theoretical elastic constants of Al_3Zr (DO23) [38,39], Zr [38,40,41] and Al [38,40,41] at zero pressure in Table 2 for comparison. The mechanical anisotropy of Zr_2Al can be calculated using the bulk moduli along the a- and c-axes, B_a and B_c by Eqs. (4)–(7), the calculated B_a and B_c at zero pressure are also shown in Table 2. The ratio B_a/B_c of Zr_2Al is 1.17, which is smaller than these of ZrB_2 (1.22), TiB_2 (1.54) and NbB_2 (1.43), indicating the stronger chemical bonding for Zr_2Al. The change of B_a and B_c with pressure are shown in Fig. 2. It can be seen that the ratio of B_a/B_c is decreasing as the pressure increases, indicating the mechanical behavior of Zr_2Al under zero pressure is of anisotropy

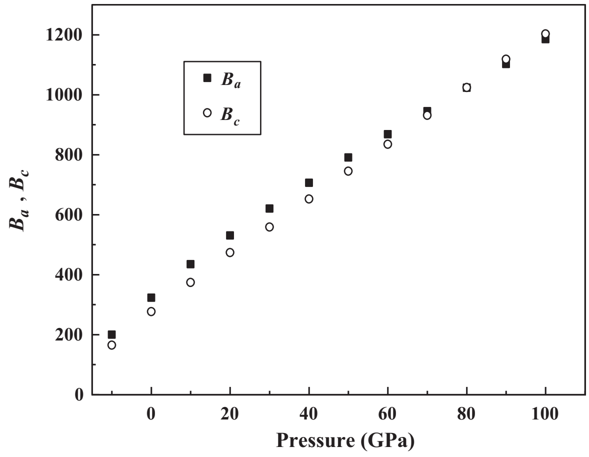

Fig. 2. The relation of the bulk modulus B_a and B_c with pressure along the a- and c-axes.

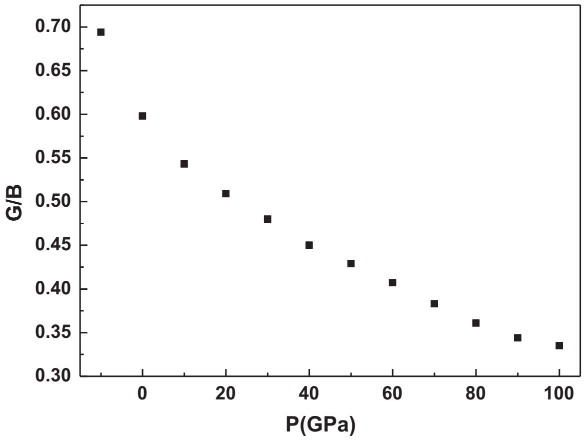

Fig. 4. The calculated quotient of G/B plotted as a function of pressure P.

Table 1
The calculated lattice parameters a, c, c/a, equilibrium volume V_0, formation energy ΔE, bulk modulus B_0 and its pressure derivative B_0' compared with experimental data and other theoretical results.

	a (Å)	c (Å)	c/a	V_0 (Å^3/atom)	ΔE (eV/atom)	B_0 (GPa)	B_0'
Present work	4.908	5.929	1.208	20.61	−0.35	102.16	3.695
Exp. [37]	4.894	5.928	1.211	20.49	–	–	–
Ref. [38]	–	–	–	20.38	–	98.10	–
Ref. [18]	–	–	–	–	−0.35 (LASTO)		
−0.37 (PWPP)	–	–					

Table 2
Five elastic constants C_{ij} (GPa) of Zr_2Al and the bulk moduli B_a and B_c (GPa) at 0 GPa and 0 K.

	C_{11}	C_{12}	C_{13}	C_{33}	C_{44}	B_a	B_c
Present	178.3	85.4	51.2	189.2	57.7	323	276
Ref. [38] Al_3Zr (DO23)	215.3	54.1	33.3	228.2	103.2	–	–
Exp. [39] Al_3Zr (DO23)	208.8	70.5	49.1	208.3	87.2	–	–
Ref. [38] Zr	153.1	63.4	76.5	171.2	22.4	–	–
Exp. [40,41] Zr (hcp)	155.4	67.2	64.6	172.5	36.3	–	–
Ref. [39] Al (fcc)	101.5	70.4	–	–	31.7	–	–
Exp. [40,42] Al (fcc)	114.3	61.9	–	–	31.6		
Exp. [43] ZrB_2	–	–	–	–	–	772	635
Exp. [44] TiB_2	–	–	–	–	–	851	553
Refs. [31,45] NbB_2	–	–	–	–	–	797	557

and the anisotropy will gradually weaken as the applied pressure increases.

The elastic constants as a function of pressure are shown in Fig. 3. It is found that the five independent elastic constants increase monotonically with pressure. C_{11} and C_{33} vary rapidly as pressure increases, C_{13} and C_{12} becomes moderate. However, C_{44} increases comparatively slowly with pressure. If this structure is stable, the five independent elastic constants should satisfy the well-known Born stability criteria [30], i.e., Eqs. (2) and (3). Fig. 3 shows excellent satisfaction of the calculated elastic constants of Zr_2Al to these equations and hence in our calculation, the Zr_2Al is mechanically stable at pressure up to 100 GPa.

The elastic moduli including the Yong's modulus E, the bulk modulus B and the shear modulus G can affect the quality of materials. As the bulk modulus B is nearly relative to the cohesive energy or bonding energy of atoms in crystals, it is used as a measure to describe the average atomic bond strength [46]. Moreover, the shear modulus G is the important parameter related to the hardness of a material [47]. The calculated polycrystalline elastic modulus and bulk modulus are shown in Table 3. Generally speaking, the larger the moduli, the harder the materials. It can be seen that from Table 3 that increasing pressure can improve the materials hardness.

Pugh [48] proposed the quotient of shear to bulk modulus of polycrystalline phases (G/B) by considering that the shear modulus G represents the resistance to plastic deformation, while the bulk modulus B represents the resistance to fracture. A high G/B ratio is associated with brittleness, while a low value corresponds to ductility. The critical value which separates ductile and brittle materials is about 0.57. If $G/B < 0.57$, the material exhibits in a ductile manner; otherwise, the material behaves in a brittle manner. Table 3 lists the values of G/B and Fig. 4 shows G/B as a function of pressure, respectively. In this study, the calculated value of G/B at 0 K and 0 GPa is 0.549, describing this material as ductile, while with the applied

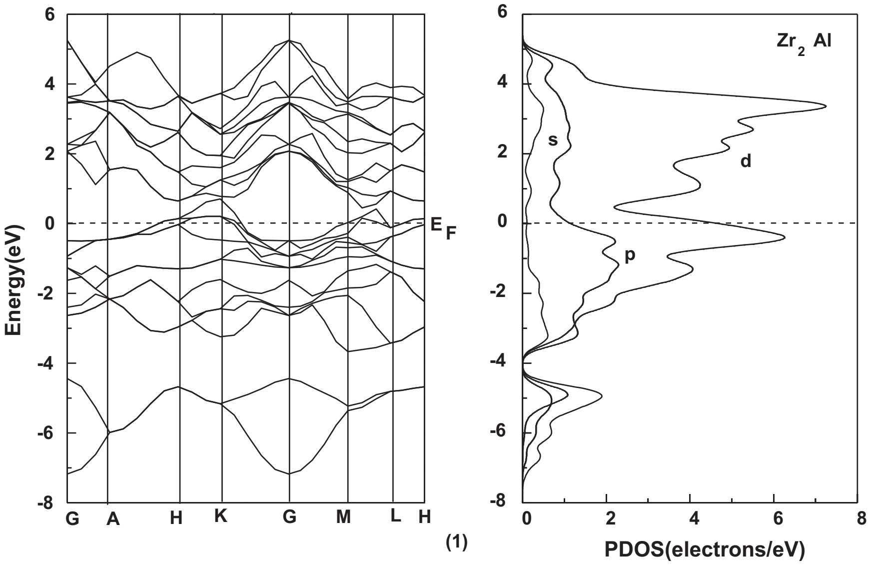

Fig. 5. Band structure and partial density of Zr_2Al at 0 K and 0 GPa.

Table 3
The Yong's modulus E (GPa), shear modulus G (GPa) and bulk modulus B (GPa) at various pressures.

P (GPa)	B_a	B_c	B	G	E	G/B
−10	200	164	62	39	96	0.629
0	323	276	102	56	142	0.549
10	434	376	138	69	178	0.500
20	531	475	171	80	207	0.468
30	620	560	200	88	231	0.44
40	705	652	229	96	252	0.419
50	792	744	259	103	273	0.398
60	866	836	285	108	288	0.379
70	945	930	313	112	299	0.358
80	1023	1026	341	115	311	0.337
90	1102	1119	369	120	324	0.325
100	1184	1204	397	125	340	0.315

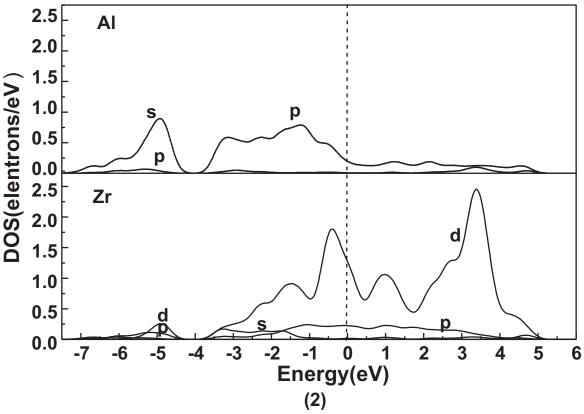

Fig. 6. The density of state of Zr and Al in Zr_2Al.

pressure increasing, the values of G/B is much more smaller, that is to say, pressure can improve the ductility of Zr_2Al.

3.3. Band structure and DOS of Zr_2Al

Band structure and the partial density of state of Zr_2Al are shown in Fig. 5. From the band structure, it can be seen that the low-lying two bands are mainly Al *s* bands and the conduction bands are hybridized bands of Zr *s*, Zr *d* and Al *p* orbitals. The lower bands in conduction state are mainly due to Zr *s* electrons, and above this a cluster of several bands is present, which are mainly contributed by Zr *d* and Al *p* orbitals. The bands which cross the Fermi level (E_F) are mainly the nonbonding states of the Zr *d* orbitals. Consequently, the major contribution to the density of states at the Fermi level is from Zr *d* electrons.

The partial density of state of Zr, Al in Zr_2Al is presented in Fig. 6. By analysis of the partial density of state (PDOS), it can be found that Al s electrons in Zr_2Al are localized and naturally do not participate in bonding. The highest peak appearing in the DOS curve is due to the bonding states which arise from the hybridization of Al *p* and Zr *d* orbitals. The sharp peak in the vicinity of the Fermi level is mainly due to the nonbonding states of the Zr *d* electrons, and therefore the physical properties of this compound could be mainly governed by Zr *d* electrons.

4. Conclusions

A detailed investigation has been performed on the structure, elastic properties and elastic anisotropy of Zr_2Al in the hcp structure using density functional theory method with the ultrasoft pseudopotential scheme in the frame of the generalized gradient approximation (GGA) under high pressure. The optimized lattice parameters are in very good agreement with the experimental data. We also investigate the heat of formation of Zr_2Al crystal and the result is in excellent consistent with results from other study. The calculated elastic constants and the bulk moduli along the crystallographic axes increase with increasing pressure. The ideal polycrystalline aggregates bulk modulus, shear modulus, and Young's modulus are investigated by Hill's approximation. From the quotient of shear to bulk modulus of polycrystalline phases (G/B), it is seen that Zr_2Al is a brittle system at low pressures and becomes ductile at higher pressures. Moreover, the ductility becomes much stronger with pressure increasing, that is to say, pressure can improve the ductility of Zr_2Al. Lastly, by analysis of band structure and the partial density of state (PDOS) of Zr_2Al, it is found that the bands which cross the Fermi level (E_F) are mainly the nonbonding states of the Zr *d* orbitals, therefore, the major contribution to the density of states at the Fermi level is from Zr *d* electrons.

Acknowledgments

This work is supported by grants from the National Natural Science Foundation of China (Grant Nos. 10776022 and 20773085), The Specialized Research Fund for the Doctoral Program of Higher Education (Grant No. 20090181110080), the State Key Laboratory of Explosion Science and Technology, Beijing Institute of Technology (Grant KFJJ09-02), the National Basic Research Program of China (Grant No. 2010CB731600), as well as, the computational resources provided by the State Key Laboratory of Polymer Materials Engineering of China in Sichuan University and the Virtual Laboratory for Computational Chemistry of CNIC, and the Supercomputing Center of CNIC, Chinese Academy of Science.

References

[1] Y.K. Vohra, P.T. Spencer, Phys. Rev. Lett. 86 (2001) 3068.
[2] Y.Q. Cheng, H.W. Sheng, E. Ma, Phys. Rev. B 78 (2008) 014207.
[3] X.F. Wu, Z.Y. Suo, Y. Si, L.K. Meng, K.Q. Qiu, J. Alloys Compd. 452 (2008) 268–272.
[4] Y.Q. Cheng, E. Ma, Appl. Phys. Lett. 93 (2008) 051910.
[5] S.E. Dang, G. Zhang, Z.Y. Li, Z.J. Yan, Y.T. Li, W. Liang, J. Alloys Compd. 479 (2009) L15–L17.
[6] S.H. Liang, J.H. Li, B.X. Liu, J. Phys. Soc. Jpn. 77 (2008) 104301.
[7] M. Stoica, N.V. Steenberge, J. Bednarčik, N. Mattern, H. Franz, J. Eckert, J. Alloys Compd. 506 (2010) 85–87.
[8] H.Z. Fang, X. Hui, G.L. Chen, Z.K. Liu, Appl. Phys. Lett. 94 (2009) 091904.
[9] M. Wencka, M. Jagodič, A. Gradišek, A. Kocjan, Z. Jagličić, P.J. McGuiness, T. Apih, Y. Yokoyama, J. Dolinšek, J. Alloys Compd. 504 (2010) 16–21.
[10] J. Guo, Y. Liu, P.X. Fan, H.X. Qu, T. Quan, J. Alloys Compd. 495 (2010) 50.
[11] A. Inoue, T. Zhang, M.W. Chen, T. Sakurai, J. Saida, M. Matsushita, J. Mater. Res. 15 (2000) 2195.
[12] H. Yang, K.Y. Lim, Y. Li, J. Alloys Compd. 489 (2010) 183–187.
[13] A. Peruzzi, J. Nucl. Mater. 186 (1992) 89.
[14] S.N. Tiwari, K. Tangri, J. Nucl. Mater. 34 (1970) 92–96.
[15] E.M. Schulson, D.H. McColl, V.C. Ling, Refinement of the Zr/Zr_2Al duplex structure in Zr-7.6 to -9.0 wt.% A1 Ingots, Chalk River Nuclear Laboratories, AECL-5176, Chalk River, Ontario, Canada, 1975.
[16] R.J. Kematick, H.F. Franzen, J. Solid State Chem. 54 (1984) 226.
[17] T. Wang, Z. Jin, J. Zhao, J. Phase Equilibria 22 (2001) 544.
[18] M. Alatalo, M. Weinert, R.E. Watson, Phys. Rev. B 57 (1998) R2009.
[19] J.P. Perdew, K. Burke, M. Ernzerhof, Phys. Rev. Lett. 77 (1996) 3865.
[20] M.C. Payne, M.P. Teter, D.C. Allen, T.A. Arias, J.D. Joannopoulos, Rev. Mod. Phys. 64 (1992) 1045.
[21] V. Milan, B. Winker, J.A. White, C.J. Packard, M.C. Payne, E.V. Akhmatskaya, R.H. Nobes, Int. J. Quantum Chem. 77 (2002) 85.
[22] P. Hohenberg, W. Kohn, Phys. Rev. 136 (1964) B864.
[23] W. Kohn, L.J. Sham, Phys. Rev. 140 (1965) A1133.
[24] R.O. Jones, O. Gunnarsson, Rev. Mod. Phys. 61 (1989) 689.
[25] R.M. Dreizler, E.K.U. Gross, Density Functional Theory—An Approach to the Quantum Many-body Problem, Springer-Verlag, Berlin, 1990.
[26] B. Mayer, H. Anton, E. Bott, M. Methfessel, J. Sticht, J. Harris, P.C. Schmidt, Intermetallics 11 (2003) 23.
[27] B.G. Pfrommer, M. CÔté, S.G. Louie, M.L. Cohen, J. Comp. Physiol. 131 (1997) 233.
[28] H.Z. Guo, X.R. Chen, L.C. Cai, J. Zhu, J. Gao, Solid State Commun. 134 (2005) 787.
[29] L. Fast, J.M. Wills, B. Johansson, O. Eriksson, Phys. Rev. B 51 (1995) 17431.
[30] M. Born, Proc. Cambridge Philos. Soc. 36 (1940) 160.

[31] A.S. Sikder, A.K.M.A. Islam, M. Nuruzzaman, F.N. Islam, Solid State Commun. 137 (2006) 253.
[32] P. Ravindran, L. Fast, P.A. Korzhavyi, B. Johansson, J. Appl. Phys. 84 (1998) 4891.
[33] W. Voigt, Lehrbook, Der Kristallphysik, 2nd ed. (Teubner, Leipsig, 1928); A. Reuss, Z. Angew. Math. Mech. 9 (1929) 49.
[34] L.L. Sun, Y. Cheng, G.F. Ji, J. At. Mol. Sci. 1 (2010) 143.
[35] R. Hill, Proc. R. Soc. Lond. Ser. A 65 (1952) 350.
[36] F.D. Murnaghan, Proc. Natl. Acad. Sci. U.S.A. 30 (1944) 244.
[37] C.G. Wilson, D. Sams, Acta. Cryst. 14 (1961) 71.
[38] E. Clouet, J.M. Sanchez, C. Sighi, Phys. Rev. B 65 (2002) 094105.
[39] M. Nakamura, K. Kimura, J. Mater. Sci. 26 (1991) 2208.
[40] R. Bechmann, R.F.S. Headmon, in: K.H. Hellwege, A.M. Hellwege (Eds.), Landolt-Börnstein, vol. III/1, Springer, Berlin, 1996.
[41] E.S. Fisher, C.J. Renken, Phys. Rev. 135 (1964) 482.
[42] G.N. Kamm, G.A. Alers, J. Appl. Phys. 35 (1964) 327.
[43] N.L. Okamoto, M. Kusakari, K. Tanaka, H. Inui, M. Yamaguchi, S. Otani, J. Appl. Phys. 93 (2003) 88.
[44] P.S. Spoor, J.D. Maynard, M.J. Pan, D.J. Green, J.R. Hellmann, T. Tanaka, Appl. Phys. Lett. 70 (1997) 1959.
[45] A.K.M.A. Islam, A.S. Sikder, F.N. Islam, Phys. Lett. A. 350 (2006) 288.
[46] K.A. Gschneidner, Solid State Phys. 16 (1964) 275.
[47] I.N. Frantsevich, F.F. Voronor, S.A. Bokuta, in: I.N. Frantsevich (Ed.), Elastic constants and elastic moduli of metals and insulators, Naukova Dumka, Kiev, 1983, p. 60.
[48] S.F. Pugh, Philos. Mag. 45 (1954) 823.